

Supplemental material: Phonon order and reststrahlen bands of polar vibrations in crystals with monoclinic symmetry

Mathias Schubert,^{1,2,3,4,*} Alyssa Mock,^{3,4} Rafał Korlacki,¹ and Vanya Darakchieva^{3,4}

¹*Department of Electrical and Computer Engineering, University of Nebraska-Lincoln, Lincoln, Nebraska 68588, U.S.A.*

²*Leibniz Institute for Polymer Research, Dresden, Germany*

³*Terahertz Materials Analysis Center, Department of Physics, Chemistry and Biology, Linköping University, SE 58183, Linköping, Sweden*

⁴*Center for III-Nitride Technology C3NiT - Janzén, Linköping University, SE 58183, Linköping, Sweden*

(Dated: December 20, 2018)

We show the derivation of equations used in our publication which lead to the identification of inner and outer phonon modes with eigenpolarization directions within the monoclinic plane, and the shape and polarization dependence of the reststrahlen bands for monoclinic symmetry materials with polar vibrations. We provide additional details of our density functional theory calculations. The case of monoclinic crystal structure gallium oxide is considered as an example.

CONTENTS

I. Coordinate systems	1
II. The eigendielectric displacement vector summation approach	2
III. The eigendielectric loss displacement vector summation approach	2
IV. The TO mode parameter set and the LO mode parameter set	2
V. Eigenmodes (eigenpolarization) and principle indices of refraction	3
VI. Total reflection conditions	3
VII. The p and q parameters, and n_{\pm}	3
VIII. Mode duality	4
IX. TO-mode reflectance band boundaries	4
X. LO-mode reflectance band boundaries	4
XI. Generalized displacement vector	4
XII. Inner and outer phonon modes and phonon mode order in monoclinic plane	5
A. Outer modes	5
B. Inner modes	5
XIII. Bands of total reflection	5
A. Unpolarized bands of total reflection	5
B. Polarized bands of total reflection	5

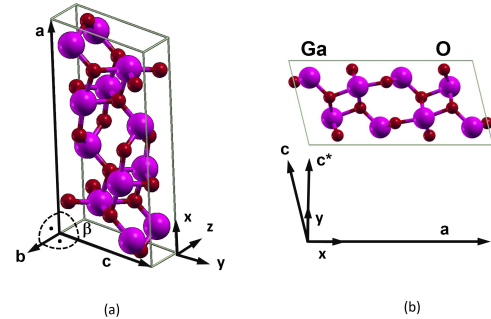


FIG. 1. (a) Definition of Cartesian laboratory coordinate system (x, y, z) , and as an example the unit cell of β -Ga₂O₃ with monoclinic angle β , and crystal unit axes \mathbf{a} , \mathbf{b} , \mathbf{c} . (b) Monoclinic plane \mathbf{a} - \mathbf{c} viewed along axis \mathbf{b} . (\mathbf{b} points into the plane.) Vector \mathbf{c}^* parallel to axis y is used for convenience. Reprinted from Ref. [1] with copyright permission by American Physical Society.

C. Polarization angle at boundaries of polarized bands of total reflection	6
XIV. Details of Density Functional Theory Calculations	7
References	8

I. COORDINATE SYSTEMS

We select a (right-handed) system of Cartesian coordinates, (x, y, z) , and place within a (right-handed) lattice axis system for a monoclinic crystal structure such that axis \mathbf{a} is parallel to x , axis \mathbf{b} is parallel to z , and axis \mathbf{c} is within the (x, y) plane. Figure 1, reproduced from Schubert *et al.*[1], reflects our selection for the example of monoclinic gallium oxide.

* schubert@engr.unl.edu; <http://ellipsometry.unl.edu>

II. THE EIGENDIELECTRIC DISPLACEMENT VECTOR SUMMATION APPROACH

The eigendielectric displacement vector summation approach describes the effect of polar vibrations onto the long-wavelength dependence of the dielectric function tensor, ε , regardless of symmetry.[1–4] The approach is equivalent to the microscopic Born-Huang description of N polar lattice vibrations in the harmonic approximation[5, 6]

$$\varepsilon = \varepsilon_\infty + \sum_{l=1}^N \frac{A_{\text{TO},l}^2}{\omega_{\text{TO},l}^2 - \omega^2} (\hat{\mathbf{e}}_{\text{TO},l} \otimes \hat{\mathbf{e}}_{\text{TO},l}), \quad (1)$$

where $A_{\text{TO},l}$, $\omega_{\text{TO},l}$, and $\hat{\mathbf{e}}_{\text{TO},l}$ are amplitude, transverse optical (TO) mode frequency, and unit eigen dielectric displacement vector of polar lattice mode l , respectively, ε_∞ is the dielectric tensor contribution due to the combined vacuum permittivity and due to higher-frequency electronic dielectric polarization, \otimes is the dyadic product, and ω is the time-harmonic frequency. Note that broadening is ignored. In this summation, all modes within the monoclinic plane have a unit vector

$$\hat{\mathbf{e}}_{\text{TO},l} = (\cos \alpha_{\text{TO},l}, \sin \alpha_{\text{TO},l}, 0). \quad (2)$$

The eigendielectric displacement unit vector for all TO modes polarized perpendicular to the monoclinic plane is

$$\hat{\mathbf{e}}_{\text{TO},l} = (0, 0, 1). \quad (3)$$

The sum includes all N TO modes within the crystal. For monoclinic gallium oxide, the sum contains 8 modes polarized within the monoclinic plane, and 4 modes perpendicular to the monoclinic plane.

III. THE EIGENDIELECTRIC LOSS DISPLACEMENT VECTOR SUMMATION APPROACH

A statement for ε^{-1} can be formulated similar to ε , then expressed with parameters for all longitudinal optical (LO) modes exchanging all labels “TO” with “LO” accordingly.[4]

$$\varepsilon^{-1} = \varepsilon_\infty^{-1} - \sum_{l=1}^N \frac{A_{\text{LO},l}^2}{\omega_{\text{LO},l}^2 - \omega^2} (\hat{\mathbf{e}}_{\text{LO},l} \otimes \hat{\mathbf{e}}_{\text{LO},l}), \quad (4)$$

where $A_{\text{LO},l}$, $\omega_{\text{LO},l}$, and $\hat{\mathbf{e}}_{\text{LO},l}$ are amplitude, LO mode frequency, and unit eigen dielectric displacement vector of polar lattice mode l , respectively. Note that broadening is ignored. In this summation, all modes within the monoclinic plane have a unit vector

$$\hat{\mathbf{e}}_{\text{LO},l} = (\cos \alpha_{\text{LO},l}, \sin \alpha_{\text{LO},l}, 0). \quad (5)$$

The eigendielectric displacement unit vector for all LO modes polarized perpendicular to the monoclinic plane is

$$\hat{\mathbf{e}}_{\text{LO},l} = (0, 0, 1). \quad (6)$$

The sum includes all N LO modes within the crystal. For monoclinic gallium oxide without free charge carriers, the sum contains 8 modes polarized within the monoclinic plane, and 4 modes perpendicular to the monoclinic plane.

IV. THE TO MODE PARAMETER SET AND THE LO MODE PARAMETER SET

Two eigenmode sets are determined by the TO and LO phonon mode properties, except for constant contributions from higher energy electronic polarizations (ε_∞), and Eqs. 1 and 4 describe the same physical processes. TO modes occur at frequencies at which dielectric resonance occurs for electric fields along $\hat{\mathbf{e}}_l$ with eigendielectric displacement unit vectors then defined as $\hat{\mathbf{e}}_l = \hat{\mathbf{e}}_{\text{TO},l}$. Similarly, LO modes occur when the dielectric loss approaches infinity for electric fields along $\hat{\mathbf{e}}_l$ with eigendielectric displacement unit vectors then defined as $\hat{\mathbf{e}}_l = \hat{\mathbf{e}}_{\text{LO},l}$. This can be written as:

$$|\det\{\varepsilon(\omega = \omega_{\text{TO},l})\}| \rightarrow \infty, \quad (7a)$$

$$|\det\{\varepsilon^{-1}(\omega = \omega_{\text{LO},l})\}| \rightarrow \infty, \quad (7b)$$

$$\varepsilon^{-1}(\omega = \omega_{\text{TO},l})\hat{\mathbf{e}}_{\text{TO},l} = 0, \quad (7c)$$

$$\varepsilon(\omega = \omega_{\text{LO},l})\hat{\mathbf{e}}_{\text{LO},l} = 0, \quad (7d)$$

where l is an index for multiple frequencies in the sets.[2] We state here without further proof that the number of TO modes must always equal the number of LO modes.

The two parameter sets are not independent from each other, and for example, if the TO mode parameters are known, the LO mode parameter set can be calculated using Eqs. 7. The LO modes follow from obtaining the roots of the determinant of Eq. 1. The LO orientation parameters for the monoclinic plane follow from Eq. 7d:

$$\tan \alpha_{\text{LO},l} = -\frac{\varepsilon_{xx}(\omega_{\text{LO},l})}{\varepsilon_{xy}(\omega_{\text{LO},l})} = -\frac{\varepsilon_{xy}(\omega_{\text{LO},l})}{\varepsilon_{yy}(\omega_{\text{LO},l})}. \quad (8)$$

The amplitude parameters for the LO mode set can be obtained from Eq. 7c, with the following equation system

$$A = M^{-1}C, \quad (9)$$

with vector components for A and C

$$(A_j) = (A_{\text{LO},j}^2), \quad (10)$$

$$(C_j) = (\varepsilon_{xy,\infty}^{-1} + \varepsilon_{yy,\infty}^{-1} \tan \alpha_{\text{TO},j}), \quad (11)$$

and matrix components for M

$$(M_{jk}) = \left(\frac{\sin \alpha_{\text{LO},j} \cos \alpha_{\text{LO},j} + \sin^2 \alpha_{\text{LO},j} \tan \alpha_{\text{TO},k}}{\omega_{\text{LO},j}^2 - \omega_{\text{TO},k}^2} \right). \quad (12)$$

The indices j and k run from 1 to N .

V. EIGENMODES (EIGENPOLARIZATION) AND PRINCIPLE INDICES OF REFRACTION

An eigenpolarization reflectance analysis can be used to study the connection between polar phonon modes in materials with monoclinic symmetry and their reststrahlen bands. Here we study the reflectance characteristics versus orbital frequency ω and linear polarization direction of an electromagnetic plane wave incident normal onto the monoclinic plane. The eigenpolarizations (electric field phasors), \mathbf{E}_{\pm} , and their corresponding wave propagation constants, n_{\pm} (principle indices of refraction) can be found from the characteristic wave equation. The electromagnetic field wave vector is $\mathbf{k} = k_0(k_x, k_y, k_z)$. Hence,

$$[\varepsilon_{ij} - n^2(\delta_{ij} - k_i k_j)] E_j = 0, \quad (13)$$

where δ_{ij} is the Kronecker symbol, $k_0 = \frac{\omega}{c}$, and c is the speed of light. For light at normal incidence to the $\mathbf{a} - \mathbf{c}$ plane ($k_x = k_y = 0$), the principle indices of refraction are

$$n_{\pm} = \frac{1}{2} \sqrt{p \pm q}, \quad (14)$$

where

$$p = \varepsilon_{xx} + \varepsilon_{yy}, \quad q = \sqrt{(\varepsilon_{xx} - \varepsilon_{yy})^2 + 4\varepsilon_{xy}^2}. \quad (15)$$

The eigenpolarizations are

$$\mathbf{E}_{\pm} = \left(\frac{\varepsilon_{xx} - \varepsilon_{yy} \pm q}{2\varepsilon_{xy}}, 1, 0 \right). \quad (16)$$

VI. TOTAL REFLECTION CONDITIONS

The reflectance coefficients, r_{\pm} , for the normal incidence eigenpolarization (\mathbf{E}_{\pm}) can be expressed through the indices of refraction n_{\pm}

$$r_{\pm} = \frac{n_{\pm} - 1}{n_{\pm} + 1}. \quad (17)$$

It is of interest for analysis of the structure of the reststrahlen band to identify conditions for total reflectance. Schubert, Tiwald and Herzinger[7] identified conditions for bands of total reflection for high-symmetry orientations of surfaces cut from materials with orthorhombic and higher symmetry. The same considerations hold for Eq. 17. Total reflection is defined by

$$\sqrt{r_{\pm} r_{\pm}^*} = 1. \quad (18)$$

where $*$ denotes the complex conjugate. Hence,

$$r_{\pm} = \sqrt{\left(\frac{n_{\pm} - 1}{n_{\pm} + 1} \right) \left(\frac{n_{\pm}^* - 1}{n_{\pm}^* + 1} \right)}, \quad (19)$$

$$r_{\pm} = \sqrt{\frac{n_{\pm} n_{\pm}^* - n_{\pm} - n_{\pm}^* + 1}{n_{\pm} n_{\pm}^* + n_{\pm} + n_{\pm}^* + 1}}. \quad (20)$$

$$r_{\pm} = \sqrt{\frac{\text{Re}\{n_{\pm}\}^2 + \text{Im}\{n_{\pm}\}^2 - 2\text{Re}\{n_{\pm}\} + 1}{\text{Re}\{n_{\pm}\}^2 + \text{Im}\{n_{\pm}\}^2 + 2\text{Re}\{n_{\pm}\} + 1}}, \quad (21)$$

$$r_{\pm} = \sqrt{\frac{\text{Im}\{n_{\pm}\}^2 + (\text{Re}\{n_{\pm}\} - 1)^2}{\text{Im}\{n_{\pm}\}^2 + (\text{Re}\{n_{\pm}\} + 1)^2}}. \quad (22)$$

Hence, $r_{\pm} = 1$ regardless of $\text{Im}\{n_{\pm}\}$ when $\text{Re}\{n_{\pm}\} = 0$, i.e.,

$$\sqrt{r_{\pm} r_{\pm}^*} = 1 \Leftrightarrow \text{Re}\{n_{\pm}\} = 0, \quad (23)$$

There are two boundaries of interest, one for which $\text{Im}\{n_{\pm}\} \rightarrow \infty$ and one for which $\text{Im}\{n_{\pm}\} \rightarrow 0$. As will be shown below, the former is associated with a TO mode, and the latter is associated with an LO mode.

VII. THE p AND q PARAMETERS, AND n_{\pm}

Coefficients p and q can be expressed by elements of Eq. 1.

$$p = (\varepsilon_{\infty,xx} + \varepsilon_{\infty,yy}) + \sum_{l=1}^N \frac{A_{\text{TO},l}^2}{\omega_{\text{TO},l}^2 - \omega^2}, \quad (24)$$

$$q = \sqrt{\left[\varepsilon_{\infty,xx} - \varepsilon_{\infty,yy} + \sum_{l=1}^N \frac{A_{\text{TO},l}^2 \cos(2\alpha_{\text{TO},l})}{\omega_{\text{TO},l}^2 - \omega^2} \right]^2 + \left[2\varepsilon_{\infty,xy} + \sum_{l=1}^N \frac{A_{\text{TO},l}^2 \sin(2\alpha_{\text{TO},l})}{\omega_{\text{TO},l}^2 - \omega^2} \right]^2}. \quad (25)$$

It is obvious from Eqs. 24 and 25 that, depending on ω ,

- (i) q is real-valued, and can be positive, or zero, but not negative.
- (ii) p is real-valued, and can be positive, zero, or negative. Note that p does not depend on $\alpha_{\text{TO},l}$.

Hence, from Eq. 14

- (iii) n_{\pm} can only be either a purely real-valued number, zero, or a purely imaginary-valued number.
- (iv) n_+ is purely real-valued when $p + q > 0$, and n_- is purely real-valued when $p - q > 0$.
- (v) n_+ is purely imaginary-valued when $p + q < 0$, and n_- is purely imaginary-valued when $p - q < 0$.
- (vi) n_+ is zero when $p + q = 0$, and n_- is zero when $p - q = 0$.
- (vii) Eigenpolarizations, \mathbf{E}_{\pm} , are linearly polarized, regardless of ω .

VIII. MODE DUALITY

While shown in more detail below, it can be already stated here that 2 types (\pm) of TO and LO modes exist, one type associated with $r_- = 1$ and one associated with $r_+ = 1$. We refer to those as XO_- and XO_+ , respectively, where ‘X’ stands for ‘T’, or ‘L’.

IX. TO-MODE REFLECTANCE BAND BOUNDARIES

When ω approaches $\omega_{\text{TO},l}$ it follows that $\det(\varepsilon_{ij}) \rightarrow +\infty$, and hence $\text{Re}\{n_{\pm}\} \rightarrow +\infty$ and $\text{Im}\{n_{\pm}\} \rightarrow 0$. Thereby, $r_{\pm} \rightarrow 1$. When ω becomes slightly larger than $\omega_{\text{TO},l}$ it follows that $|\det(\varepsilon_{ij})| \rightarrow \infty$, and hence $\text{Im}\{n_{\pm}\} \rightarrow +\infty$ and $\text{Re}\{n_{\pm}\} = 0$. Then, $r_{\pm} = 1$. This change appears across an infinitesimally small frequency range at $\omega_{\text{TO},l}$, and thus marks the frequencies of TO modes.

X. LO-MODE REFLECTANCE BAND BOUNDARIES

When $\omega = \omega_{\text{LO},l}$ it follows that $\det(\varepsilon_{ij}) = 0$, $n_{\pm} = 0$, and hence $r_{\pm} = 1$. This is shown in the following:

$$n_{\pm} = \frac{1}{2} \sqrt{\varepsilon_{xx} + \varepsilon_{yy} \pm \sqrt{(\varepsilon_{xx} - \varepsilon_{yy})^2 + 4\varepsilon_{xy}^2}}. \quad (26)$$

For $\omega = \omega_{\text{LO}}$,

$$0 = \varepsilon_{xx}\varepsilon_{yy} - \varepsilon_{xy}^2, \quad (27)$$

hence,

$$n_{\pm} = \frac{1}{2} \sqrt{\varepsilon_{xx} + \varepsilon_{yy} \pm \sqrt{(\varepsilon_{xx} + \varepsilon_{xx})^2}}. \quad (28)$$

Because the term $\sqrt{(\dots)^2}$ is always positive, there are two cases for $\omega_{\text{LO},l}$. When $(\varepsilon_{xx} + \varepsilon_{yy}) < 0$

$$n_+ = 0 \leftrightarrow \omega = \omega_{\text{LO},+}, \quad (29)$$

and when $(\varepsilon_{xx} + \varepsilon_{yy}) > 0$

$$n_- = 0 \leftrightarrow \omega = \omega_{\text{LO},-}. \quad (30)$$

Hence, the condition for reflectance approaching unity at which both the real and the imaginary parts of the index n_{\pm} vanish coincides with frequencies of LO modes. Note that inspecting $(\varepsilon_{xx} + \varepsilon_{yy})$ at a given LO mode permits identification of its “+” or “-” character, and which we further down define as inner or outer mode character, respectively.

XI. GENERALIZED DISPLACEMENT VECTOR

We introduce a vector, \mathbf{q} , and present it as a generalized displacement vector, described within the $\mathbf{a} - \mathbf{c}$ plane. First, for convenience of writing, we include the contributions to the dielectric function due to higher-energy polarizabilities, the constant ε_{∞} , as dyadic products. Tensor ε_{∞} is characterized by 3 real-valued quantities, $\varepsilon_{\infty,xx}$, $\varepsilon_{\infty,yy}$, and $\varepsilon_{\infty,xy}$. We can write this tensor as the sum of 2 independent dyadic forms

$$\varepsilon_{\infty} = \sum_{l=N+1}^{N+2} \varepsilon_{\infty,l} (\hat{\mathbf{e}}_{\text{TO},l} \otimes \hat{\mathbf{e}}_{\text{TO},l}). \quad (31)$$

The number of free parameters (4) in Eq. 31 exceeds the number of parameters (3) needed to render ε_{∞} , and one can choose, for example, the dyadic vector $\hat{\mathbf{e}}_{\text{TO},N+2}$ to be parallel to y , i.e., $\hat{\mathbf{e}}_{\text{TO},N+2} = (0, 1, 0)$. Then we can write the vector \mathbf{q} as a sum of vector functions, \mathbf{q}_l

$$\mathbf{q} = \sum_{l=1}^{N+2} \mathbf{q}_l, \quad (32)$$

with vector functions, \mathbf{q}_l

$$\mathbf{q}_l = q_l [\sin(2\alpha_{\text{TO},l}) \hat{\mathbf{e}}_x + \cos(2\alpha_{\text{TO},l}) \hat{\mathbf{e}}_y], \quad (33)$$

and coordinate functions, q_l

$$q_l = \frac{A_{\text{TO},l}^2}{\omega_{\text{TO},l}^2 - \omega^2}, \quad (34)$$

for $l = 1, \dots, N$, and

$$\mathbf{q}_{N+1} = q_{N+1}[\sin(2\alpha_{\text{TO},N+1})\hat{\mathbf{e}}_x + \cos(2\alpha_{\text{TO},N+1})\hat{\mathbf{e}}_y], \quad (35)$$

$$\mathbf{q}_{N+2} = q_{N+2}[\sin(2\alpha_{\text{TO},N+2})\hat{\mathbf{e}}_x + \cos(2\alpha_{\text{TO},N+2})\hat{\mathbf{e}}_y], \quad (36)$$

and

$$q_{N+1} = \varepsilon_{\infty,1}, \quad (37)$$

$$q_{N+2} = \varepsilon_{\infty,2}. \quad (38)$$

We note now that the sum of all coordinate functions of all thereby defined vector functions, \mathbf{q}_l , is identical with p defined in Eq. 24

$$\sum_{l=1}^{N+2} q_l = p, \quad (39)$$

where the individual components of the sum, vector functions q_l , can be positive, negative, or zero.

We further note that the formal vector magnitude of \mathbf{q} is then identical with q in Eq. 25

$$\sqrt{\sum_{l=1}^{N+2} q_l^2} = q. \quad (40)$$

Vector \mathbf{q} is a virtual construct, and does not exist as a physical quantity. However, its magnitude, q , can be interpreted as the total sum over all dielectric displacement produced by all lattice modes at a given frequency ω , and the direction of a given displacement is disregarded. All displacements are added positively. Regardless of ω , there is always a positive total displacement. On the other hand, the sum of the individual displacements, p , can be interpreted as net displacement at a given frequency ω . While some mode(s) may display positive displacement ($\omega^2 < \omega_{\text{TO},l}^2$), other mode(s) may display negative displacement ($\omega^2 > \omega_{\text{TO},l}^2$), and depending on ω , amplitude, and frequency parameters of all TO modes, the net displacement is negative, zero, or positive. Thereby, q and p permit comparison between total displacement with net displacement, respectively, and depending on which is larger or smaller, the signature (real-valued or imaginary-valued) of the principle indices of refraction, n_{\pm} is obtained, and phonon mode character and band assignments can be made accordingly. The factor 2 occurring in the angular unit vector arguments in Eq. 32 has no physical meaning because the mathematical orientation of vector \mathbf{q} within the monoclinic plane is deemed here irrelevant.

XII. INNER AND OUTER PHONON MODES AND PHONON MODE ORDER IN MONOCLINIC PLANE

Two cases emerge from Eq. 23

$$\sqrt{r_- r_-^*} = 1 \Leftrightarrow p - q \leq 0, \quad (41)$$

and

$$\sqrt{r_+ r_+^*} = 1 \Leftrightarrow p + q \leq 0. \quad (42)$$

A. Outer modes

Equation 41 constitutes bands of total reflection across frequency regions of what we define “outer modes”. The net displacement is smaller than the total displacement. With increasing frequency the band in r_- begins at a TO_- mode and extends to a thereby associated mode LO_- . We arrange these modes into pairs: $[\text{TO}_{j,-}, \text{LO}_{j',-}]$.

B. Inner modes

Equation 42 constitutes bands of total reflection across frequency regions of what we define “inner modes”. The net displacement (p) is negative and larger than the total displacement $q > 0$. With increasing frequency the band in r_+ begins at a TO_+ mode and extends to a thereby associated mode LO_+ . We arrange these modes into pairs: $[\text{TO}_{j,+}, \text{LO}_{j',+}]$.

XIII. BANDS OF TOTAL REFLECTION

A. Unpolarized bands of total reflection

Total unpolarized reflection occurs when light is totally reflected regardless of polarization. This is the case when $r_- = r_+ = 1$. When $p + q < 0$ (condition for inner mode spectral region), and because of $q > 0$ always, then also $p - q < 0$ (condition for outer mode) and, hence, $r_+ = r_- = 1$. Thus, within frequencies of inner mode pairs, $[\text{TO}_{j,+}, \text{LO}_{j',+}]$, one observes polarization independent total reflection. Such will form bands (parallel streaks versus rotation), for example, when reflectance is plotted as a function of wavelength and as a function of the linear incident light polarization direction relative to a direction within the monoclinic plane. This is shown as example for $\beta\text{-Ga}_2\text{O}_3$ in Fig. 2 of our paper.

B. Polarized bands of total reflection

Within spectral regions inside outer mode pairs not overlaid by inner mode pairs, $[\text{TO}_-, \text{LO}_-] \cap [\text{TO}_+, \text{LO}_+]$,

total reflection occurs only when $r_- = 1$, hence, for polarization \mathbf{E}_- only. We refer to these bands as polarization (or angular) dependent bands. These bands consist of narrow lines in a frequency versus linear polarization angle diagram along which total reflectance occurs. There are three types of these bands, characterizing those in ascending order of frequency by

- (I) bands of type I between modes $\text{TO}_- \dots \text{LO}_-$, i.e., within an outer mode pair not interrupted by an inner mode pair,
- (II) bands of type II between modes $\text{TO}_- \dots \text{TO}_+$, i.e., beginning at an outer mode and ending at and inner mode,
- (III) bands of type III between modes $\text{LO}_+ \dots \text{TO}_+$, i.e., from the end of an inner mode pair to the begin of the next inner mode pair residing within the same outer mode pair, and
- (IV) bands of type IV between modes $\text{LO}_+ \dots \text{LO}_-$, i.e., from the end of an inner mode pair to the end of an outer mode pair.

Occurrences of all such bands are shown in Fig. 2 in our paper for the example of $\beta\text{-Ga}_2\text{O}_3$. Note that for $\beta\text{-Ga}_2\text{O}_3$ we find 1, 2, 3, and 2 polarized bands of total reflection of type I, II, III, and IV, respectively.

C. Polarization angle at boundaries of polarized bands of total reflection

The lines of total reflection begin and end at frequencies and directions of the modes in $[\text{TO}_-, \text{LO}_-] \cap [\text{TO}_+, \text{LO}_+]$. There are 4 cases

- $\omega = \omega_{\text{TO}_{j,-}}$: The begin of a polarized band where $r_- = 1$, and the polarized band can be of type I (within an outer mode pair without inner mode pairs), or of type II (beginning at an outer mode TO and ending at an inner mode TO);
- $\omega = \omega_{\text{LO}_{j,-}}$: The end of a polarized band where $r_- = 1$ of type I, or of type IV (beginning at an inner mode LO and ending at an outer mode LO).
- $\omega = \omega_{\text{TO}_{j,+}}$: The end of a band where $r_- = 1$ and onset of unpolarized band of total reflections since $r_+ = 1$. Band ending is of type II, or of type III (beginning at inner LO and ending at next inner mode TO);
- $\omega = \omega_{\text{LO}_{j,+}}$: The begin of a polarized band where $r_- = 1$ of type III, or the end of a polarized band where $r_- = 1$ of type IV.

The angular parameters, at which the polarized bands of total reflection begin and end can be directly read

from the directions of the eigenvectors. For the polarized bands, $r_- = 1$, and the relevant vector whose polarization direction we follow here is \mathbf{E}_- . The relevant information is the angular orientation of the linear polarization of the eigenvector within the monoclinic plane, evaluated at the frequencies $\omega_{\text{TO}_{j,-}}$, $\omega_{\text{TO}_{j,+}}$, $\omega_{\text{LO}_{j,+}}$, and $\omega_{\text{LO}_{j,-}}$:

$$\varphi_- = \tan^{-1}(E_{-,y}/E_{-,x}), \quad (43)$$

$$\varphi_- = \tan^{-1}\left(\frac{2\varepsilon_{xy}}{\varepsilon_{xx} - \varepsilon_{yy} - q}\right). \quad (44)$$

We begin with the angular parameters of the linear eigenpolarization at the LO mode frequencies. Because $n_{\pm} = 0$ at the frequency of an LO mode, we therefore note that

$$\omega = \omega_{\text{LO}_{j,+}} \rightarrow q = -p, \quad (45)$$

and

$$\omega = \omega_{\text{LO}_{j,-}} \rightarrow q = p. \quad (46)$$

Recalling that $p = \varepsilon_{xx} + \varepsilon_{yy}$, we can see that

$$\varphi_-(\omega_{\text{LO}_{j,+}}) = \tan^{-1}\left(\frac{\varepsilon_{xy}}{\varepsilon_{xx}}\right) = \alpha_{\text{LO}_{j,+}} \pm \frac{\pi}{2}, \quad (47)$$

and

$$\varphi_-(\omega_{\text{LO}_{j,-}}) = \tan^{-1}\left(-\frac{\varepsilon_{xy}}{\varepsilon_{yy}}\right) = \alpha_{\text{LO}_{j,-}}. \quad (48)$$

The former is the cotangent and the latter is the tangent of the LO mode eigenvector angular parameter, which becomes clear when comparing with the definition of the LO mode eigenvector in Eq. 7. Hence, the polarized bands of reflection end at the angular orientation of the LO mode for outer (-) modes, and perpendicular to the orientation of the LO mode for an inner (+) mode. This can be inspected, for example, in Fig. 2 of our paper, where the polarized bands of total reflection connect to the angular orientation of the LO_- modes, or to perpendicular orientations of the LO_+ modes. The LO modes are depicted by squares. Closed squares are the eigenvector orientations. Open squares are shifted away from the closed squares along the abscissa by $\pm \frac{\pi}{2}$ to indicate the perpendicular position of the eigenvectors.

Next we investigate the angular parameters of the linear eigenpolarization at the TO frequencies. The structure of Eq. 44 can be simplified substantially when ω approaches one of the frequencies of the TO modes. We introduce tensor amplitude factors, f_i

$$f_j = \frac{A_{\text{TO},j}^2}{\omega_{\text{TO},j}^2 - \omega^2}. \quad (49)$$

Note that factors for $N+1$ ($\varepsilon_{\infty, N+1}$) and $N+2$ ($\varepsilon_{\infty, N+1}$) are wavelength independent. Now we can rewrite the angular parameters, and note that the amplitude factor

belonging to a given TO mode j , f_j , is growing over all other amplitude parameters, and which thus can be ignored:

$$\varphi_-(\omega) = \tan^{-1} \left(\frac{2 \sum f_j \sin \alpha_j \cos \alpha_j}{\sum f_j \cos^2 \alpha_j - \sum f_j \sin^2 \alpha_j - \sqrt{(\sum f_j \cos^2 \alpha_j - \sum f_j \sin^2 \alpha_j)^2 + 4 (\sum f_j \sin \alpha_j \cos \alpha_j)^2}} \right), \quad (50)$$

$$\varphi_-(\omega \rightarrow \omega_{\text{TO}_{j,\pm}}) = \tan^{-1} \left(\frac{2f_j \sin \alpha_j \cos \alpha_j}{f_j \cos^2 \alpha_j - f_j \sin^2 \alpha_j - \sqrt{(f_j \cos^2 \alpha_j - f_j \sin^2 \alpha_j)^2 + 4 (f_j \sin \alpha_j \cos \alpha_j)^2}} \right), \quad (51)$$

$$\varphi_-(\omega \rightarrow \omega_{\text{TO}_{j,\pm}}) = \tan^{-1} \left(\frac{2f_j \sin \alpha_j \cos \alpha_j}{f_j \cos^2 \alpha_j - f_j \sin^2 \alpha_j - \sqrt{(f_j \cos^2 \alpha_j + f_j \sin^2 \alpha_j)^2}} \right), \quad (52)$$

$$\varphi_-(\omega \rightarrow \omega_{\text{TO}_{j,\pm}}) = \tan^{-1} \left(\frac{2f_j \sin \alpha_j \cos \alpha_j}{f_j \cos^2 \alpha_j - f_j \sin^2 \alpha_j - |f_j|} \right). \quad (53)$$

Hence, the signature of f_j determines the outcome. With increasing frequency, bands of type I and type II begin at an outer TO mode. Approaching a mode $\omega_{\text{TO}_{j,-}}$ from frequencies slightly above (larger), the associated leading amplitude function f_j reaches negative infinity. Hence, the signature of f_j is negative. Then

$$\varphi_-(\omega \rightarrow \omega_{\text{TO}_{j,-}}) = \tan^{-1} \left(\frac{-2 \sin \alpha_j \cos \alpha_j}{-\cos^2 \alpha_j + \sin^2 \alpha_j - 1} \right) \quad (54)$$

$$\varphi_-(\omega \rightarrow \omega_{\text{TO}_{j,-}}) = \tan^{-1} \left(\frac{\sin \alpha_j}{\cos \alpha_j} \right) \quad (55)$$

$$\varphi_-(\omega \rightarrow \omega_{\text{TO}_{j,-}}) = \alpha_j = \alpha_{\text{TO}_{j,-}}. \quad (56)$$

With increasing frequency, bands of type II and type III end at an inner TO mode. Approaching a mode $\omega_{\text{TO}_{j,+}}$ from frequencies slightly below (smaller), the associated leading amplitude function f_j reaches positive infinity. Hence, the signature of f_j is positive. Then

$$\varphi_-(\omega \rightarrow \omega_{\text{TO}_{j,+}}) = \tan^{-1} \left(\frac{\cos \alpha_j}{\sin \alpha_j} \right) \quad (57)$$

$$\varphi_-(\omega \rightarrow \omega_{\text{TO}_{j,+}}) = \alpha_j \pm \frac{\pi}{2} = \alpha_{\text{TO}_{j,+}} \pm \frac{\pi}{2}. \quad (58)$$

Hence, polarized bands of total reflectance begin at outer TO mode frequencies for light polarized parallel to the TO mode orientation, and end at inner TO mode frequencies with light polarized perpendicular to the TO

mode orientation. This can be inspected, for example, in Fig. 2 of our paper, where the polarized bands of total reflection connect to the angular orientation of the TO_- modes, or to perpendicular orientations of the TO_+ modes. The TO modes are depicted by circles. Closed circles are the eigenvector orientations. Open circles are shifted along the abscissa by $\pm \frac{\pi}{2}$.

XIV. DETAILS OF DENSITY FUNCTIONAL THEORY CALCULATIONS

Density functional theory (DFT) calculations were carried out independently from the processing of experimental data. We used the open-source plane-wave code Quantum ESPRESSO.[8] While working on the current manuscript, we noticed that the sequence of LO and TO modes, and particularly the inner-outer mode pairs, derived from the calculations we published previously [1], and performed at the local density approximation level, differs in several significant details from the experimental picture. Therefore, the DFT results included here are from a different calculation at the generalized gradient approximation (GGA) level, which is otherwise identical to the one we presented in Ref. [9], which in that study we used as the starting point of hybrid band structure calculations, and for which the calculated phonon properties were not presented before.

We used exchange-correlation functional of Perdew, Burke and Ernzerhof (PBE),[10] and classic norm-conserving Troullier-Martins pseudopotentials originally generated using FHI98PP,[11, 12] available in Quantum

ESPRESSO pseudopotentials library. The pseudopotential for gallium did not include the semicore $3d$ states in the valence configuration. The dynamical matrix (including the Born effective charges) was calculated at the Γ -point of the Brillouin zone using density functional perturbation theory, [13, 14] with a tight convergence threshold for self-consistency of 10^{-18} Ry. The dynamical matrix was then processed by a post-processing code **dynmat.x** (part of the Quantum ESPRESSO distribution used for diagonalizing the dynamical matrix and computing its eigenvectors and eigenvalues). The parameters

of the TO modes were calculated by simply diagonalizing the as-obtained dynamical matrix. The limiting frequencies of the B_u modes, including direction-dependent electric field contributions, were obtained by setting the direction of approaching the Γ -point. The entire monoclinic $\mathbf{a} - \mathbf{c}$ plane was probed with a fine step of 0.01° , and the angular dependence of phonon frequencies for all eight B_u modes is presented in Fig. 1 of our publication. The LO modes were identified as extrema (minima or maxima) on the curves of limiting frequencies not coinciding with the frequencies of TO modes.

-
- [1] M. Schubert, R. Korlacki, S. Knight, T. Hofmann, S. Schöche, V. Darakchieva, E. Janzén, B. Monemar, D. Gogova, Q.-T. Thieu, R. Togashi, H. Murakami, Y. Kumagai, K. Goto, A. Kuramata, S. Yamakoshi, and M. Higashiwaki, *Phys. Rev. B* **93**, 125209 (2016).
- [2] M. Schubert, *Phys. Rev. Lett.* **117**, 215502 (2016).
- [3] A. Mock, R. Korlacki, S. Knight, and M. Schubert, *Phys. Rev. B* **95**, 165202 (2017).
- [4] A. Mock, R. Korlacki, S. Knight, and M. Schubert, *Phys. Rev. B* **97**, 165203 (2018).
- [5] M. Born and K. Huang, *Dynamical Theory of Crystal Lattices* (Clarendon, Oxford, 1954).
- [6] G. Venkataraman, L. A. Feldkamp, and V. C. Sahni, *Dynamics of Perfect Crystals* (The MIT Press, Cambridge, Massachusetts, and London, England, 1975).
- [7] M. Schubert, T. E. Tiwald, and C. M. Herzinger, *Phys. Rev. B* **61**, 8187 (2000).
- [8] Quantum ESPRESSO is available from <http://www.quantum-espresso.org>. See also: P. Giannozzi, S. Baroni, N. Bonini, M. Calandra, R. Car, C. Cavazzoni, D. Ceresoli, G. L. Chiarotti, M. Cococcioni, I. Dabo, A. D. Corso, S. de Gironcoli, S. Fabris, G. Fratesi, R. Gebauer, U. Gerstmann, C. Gougoussis, A. Kokalj, M. Lazzeri, L. Martin-Samos, N. Marzari, F. Mauri, R. Mazzarello, S. Paolini, A. Pasquarello, L. Paulatto, C. Sbraccia, S. Scandolo, G. Sclauzero, A. P. Seitsonen, A. Smogunov, P. Umari, and R. M. Wentzcovitch, *J. Phys.: Cond. Mat.* **21**, 395502 (2009).
- [9] A. Mock, R. Korlacki, C. Briley, V. Darakchieva, B. Monemar, Y. Kumagai, K. Goto, M. Higashiwaki, and M. Schubert, *Phys. Rev. B* **96**, 245205 (2017).
- [10] J. P. Perdew, K. Burke, and M. Ernzerhof, *Phys. Rev. Lett.* **77**, 3865 (1996).
- [11] M. Fuchs and M. Scheffler, *Comput. Phys. Commun.* **119**, 67 (1999).
- [12] N. Troullier and J. L. Martins, *Phys. Rev. B* **43**, 1993 (1991).
- [13] X. Gonze and C. Lee, *Phys. Rev. B* **55**, 10355 (1997).
- [14] S. Baroni, S. de Gironcoli, A. D. Corso, S. Baroni, S. de Gironcoli, and P. Giannozzi, *Rev. Mod. Phys.* **73**, 515 (2001).